

Shape-Based Functional Principal Component Monitoring of Low-Sampling-Rate CNC Machining Processes

Stephen Howard Davis^{1,*} and Frank M. White¹

¹ Walter P. Murphy Professor Emeritus of Engineering Sciences and Applied Mathematics, Northwestern University

* Correspondence: sdavis@northwestern.edu

Abstract: Typical approaches to monitoring in the machining process involve frequent readings from sensors such as vibration, acoustic emission, and cutting force sensors. In many cases, though, the sampling frequency of controller/plant historian-based spindle load signals is much lower than what is used for high frequency sensors. The focus of this paper is thus on machining-process monitoring using slow sampling spindle-load signal collected by controllers and plant historians, based on a titanium machining process in aerospace industry. For this case study, there are a total of 18 synchronized spindle loads of Program 1543, Tool 6040, and Machine T5-1, in which Run 237 and Run 241 are flagged as abnormal with onset at approximately 189 s and 303 s. These 18 spindle-load trajectories are characterized via functional principal components analysis, and are evaluated using a combination of outlier detection in the score space along with reconstruction residuals. The proposed framework allows one to retain the simplicity of using a low-rate controller for monitoring while switching from point-wise density check to trajectory-wise modeling of the machining process.

Keywords: condition monitoring; CNC machining; spindle load; low sampling rate; functional principal component analysis; anomaly detection; smart manufacturing

1. Introduction

Process monitoring has become an essential component of modern manufacturing because any anomalies in equipment behavior, tooling, and processing lead inevitably to scrap, unnecessary stoppages, and increased cost. While monitoring algorithms in the era of data-driven smart manufacturing should aim to not only identify abnormalities but also to model sufficiently well the normal process behavior to isolate any suspicious runs before they yield faulty parts [1–5].

The overwhelming majority of research into machining monitoring uses high-rate sensing. From classical to contemporary papers, vibration, cutting force, acoustic emission, motor current, or multi-sensor fusion are considered with kilohertz or even faster sampling due to their sensitivity to transient, chattering, and other wear-related phenomena [6–11]. However, this approach faces difficulties in practical implementation, which is usually limited by compatibility with existing control and history databases, lack of room for additional sensors, and heterogeneous machine pools [12–14].

Methodologically speaking, industrial low-rate monitoring has close connections with the domain of process monitoring in statistics. The contributions of principal-component-based monitoring, residual-based control schemes, multivariate batch analysis, and dynamic latent variable models proved that it is possible to reliably perform statistical surveillance using historical data when correlation structure of the process is modeled and exploited [15–25]. This body of knowledge is especially relevant in the case of low-sampled controller variables because, unlike traditional sensing approaches, they allow virtually no room for feature engineering and require exploitation of trajectory dependence and historical variation.

Citation: Stephen Howard Davis and Frank M. White. 2021. Shape-Based Functional Principal Component Monitoring of Low-Sampling-Rate CNC Machining Processes. *TK Techforum Journal (ThyssenKrupp Techforum)* 2021(3): 1–14.

Received: June-21-2021

Accepted: November-20-2021

Published: December-30-2021



Copyright: © 2021 by the authors. Licensee TK Techforum Journal (ThyssenKrupp Techforum). This article is an open access article distributed under the terms and conditions of the Creative Commons Attribution (CC BY) license (<https://creativecommons.org/licenses/by/4.0/>).

One specific instance of the problems mentioned above was addressed by Bernard et al., who studied spindle load monitoring during titanium parts manufacturing using only 1/3 Hz sampling of controller-level spindle loads. They showed that reliable process monitoring was possible at such a high sparsity level, provided repeated runs were aligned and analyzed statistically. Specifically, the previous authors developed kernel density estimation (KDE) based algorithm to identify in real time a time-dependent spindle-load distribution of normal process behavior and compare incoming runs' measurements against it. Their procedure was practical, automated, and applicable for industrial deployment, though it did face typical practical challenges associated with low-rate monitoring – e.g., heterogeneity of data, sub-program- and tool-specific effect, lack of sufficient timestamps, and proprietary and storage-constrained historical archive [26].

Pointwise density estimation has its applications in spindle-load monitoring, but this approach remains inherently local in time: it learns spindle loads that might be observed at every time-bin index but does not capture the trajectory structure, namely shape, rises and valleys, plateaus, etc. This idea of using functional modeling, in fact, appears in other density-based and even PCA-based studies of machining processes and rotating equipment: they emphasize the utility of kernel density ideas but demonstrate once again that anomaly information is distributed across the whole trajectory and not a few isolated time-bins [27]. Given the extremely sparse character of industrial low-sampled data, modeling the trajectory globally and analyzing its shape is crucially important in detecting and isolating abnormal runs.

In order to overcome the drawbacks mentioned above, the current paper applies functional principal component analysis (FPCA) and two derived monitoring statistics. Every spindle load run will be viewed not as a set of independently sampled time-bin measurements, but as a functional trajectory defined over normalized machining time. Historical normal runs are analyzed using FPCA to recover latent variation modes, which allows representing the incoming trajectories as low-dimensional score vectors and associated prediction residuals. The displacement and reconstruction information is used to compute two monitoring statistics – T^2 statistic and squared prediction error (SPE), respectively.

The motivation behind FPCA is twofold. On the one hand, functional data techniques allow capturing trajectory shapes and supporting smooth latent deformation modes – properties that make it easier to connect industrial sparsely sampled time-series data to a statistical model. On the other hand, robust principal component analysis (PCA) methods, outlier detection principles, and recent data-driven manufacturing research highlight the importance of separating usual process variation from novel structural abnormalities in the absence of large labeled archives [28–30]. These factors are even more critical on the shop-floor, where abundant but low-rate industrial datasets and the need to understand monitoring decisions go hand-in-hand.

Therefore, the current paper is concerned with the question of developing FPCA-based trajectory modeling for spindle loads in aerospace machining process monitoring and assessing its ability to discriminate between normal and abnormal trajectories on an industrial dataset. Specifically, synchronized data of controller-level traces are considered, trajectory model is proposed and evaluated based on two abnormal runs 237 and 241 of Program 1543, Tool 6040, and Machine T5-1 with their KDE scores of 47.52% and 45.34%, and respective onset times near 189 s and 303 s [31]. In addition to the problem-solving aspects, we will investigate whether such a model can be realistically applied in the low-rate environment.

The remainder of this paper is organized as follows. Section 2 introduces the dataset and the problem statement. Section 3 gives an overview of FPCA-based trajectory modeling. Section 4 contains the main findings about abnormal runs' discrimination via FPCA. Section 5 analyzes some deployment-related aspects of industrial low-rate monitoring, while the conclusion is drawn in Section 6.

2. Dataset and problem formulation

2.1. Industrial context

The data analyzed in this paper correspond to the industrial machining setup [26]. The data collection process involved collecting data from an aerospace production line, where complex titanium components were manufactured. The shop floor data infrastructure collected data from three main sources: the CNC controller, a spindle-based system responsible for tool use logging, and the spindle-based machine software containing operating condition information. The variable that is especially useful from the point of view of the controller variables is spindle load. It is an important parameter because it indicates the energy required for maintaining the spindle movement when the tool engages with the workpiece. Therefore, spindle load becomes a useful signal for cutting engagement and process deviation, in accordance with other process sensing and machining monitoring applications described in the related literature [4,5,31].

One of the most challenging aspects of the considered dataset is its acquisition frequency. Data were logged at the rate of 1/3Hz regardless of whether the machine performs an active machining operation. The sampling rate is orders of magnitude lower than what could be achieved by spindle-based or dedicated tool condition monitoring techniques. Thus, it can serve as a good benchmark for the monitoring approaches which are able to derive relevant information using a very sparse data acquisition strategy [1,2,12,26].

Figure 1 and Table 1 describe the hierarchical structure and controller-level data gathering environment of the considered runs. These data are important because the model is developed according to the same program-level grouping and tool-level classification as well as taking into account the variables of the controller interface, allowing data synchronization.

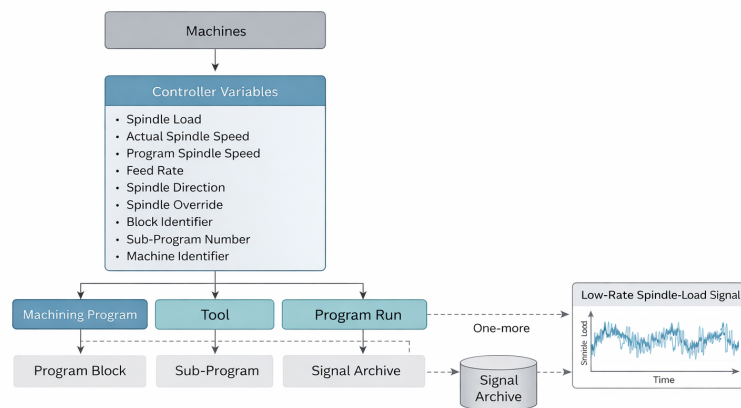


Figure 1. Relationship between machines, tools, program blocks, sub-programs, program runs, and sensor readings in the industrial machining dataset [26].

2.2. Data structure and synchronization

The data exhibit hierarchy in accordance with practical machining operations; each finished part involves multiple CNC programs, which include a number of sub-programs within themselves, and specific tools can be either reused, substituted or swapped via the sister-tool mechanism during operations. As a result, a similar nominal part production process could produce signals with great variety in the order length, local timing, and transition delay when considered based on timestamps in their raw form only. This particular problem was noted and addressed in the original study through a process of synchronization, involving reorganization of the measurements into program blocks, program runs and sequence order. This synchronization process is followed here since comparison of such processes at a low rate of sampling necessarily involves alignment of repeated program/tool combinations runs prior to building a statistical model. After

Table 1. Controller parameters recorded for the analyzed industrial machining runs [26].

Data	Units
Date	Y/M/D H:m:s:mill
Motor Coil Temperature	°C
Front Bearing Temperature	°C
Rear Bearing Temperature	°C
Actual Spindle Speed	RPM
Command Spindle Speed	RPM
Spindle Override	%
Spindle Direction	CW, CCW, STOP, ORIENTATION
Instructed Feed	[mm/min], [in./min]
Feed Override	%
Cutting Signal	ON / OFF
Jog Override	%
Rapid Override	%
Feed Signal axis	%
Relative Position	[mm], [in.], [°]
Absolute Position	[mm], [in.], [°]
Machine Position	[mm], [in.], [°]
Distance to go	[mm], [in.], [°]
Feed Load	%
NC MODE	MEMORY, MIDI, REMOTE
Spindle FTN	#
Spindle ITN	#
Main Program	#
Exec Program	#
Seq Number	#
Execution Block	G-Code
Block Counter	#
Vibration (x, y, z)	g
Spindle Load	%

synchronization, each run can be regarded as a one-dimensional spindle load trajectory in a common process coordinate system. The current example involves Program 1543 in conjunction with Tool 6040 at Machine T5-1. In total, there are 18 runs, where Runs 237 and 241 are marked as anomalous with reference analysis [26].

Figure 2 illustrates hierarchy among machining program blocks and sub-blocks of tools over time, whereas Figure 3 demonstrates synchronized spindle load trajectories of Program 1543, Tool 6040 at Machine T5-1. Figure 4 summarizes the mean and normal band extracted from this aligned set of runs.

2.3. Objectives of monitoring

The following problem was considered in the present study. Assume there exists a group of synchronous spindle-load runs of some program/program-part/tool combinations. Some/most of them are indicative of the correct operation. The goal is to build a model of spindle-load development and assess, whether the newly incoming spindle-load run should be treated as typical or non-typical for the program/program-part/tool in question. Such approach should fulfill several criteria. First, it has to function properly in the conditions of a low-frequency sampling of measurements. Second, it has to be computationally efficient in terms of memory and processing power required. Third, it cannot rely on the availability of explicit labels of faults, since most of the abnormalities in practice become known through the inspections of machined parts. Fourth, it has to be sufficiently interpretable to enable engineers understand what kind of deviation from the expected machining process led to generating an alarm [2].

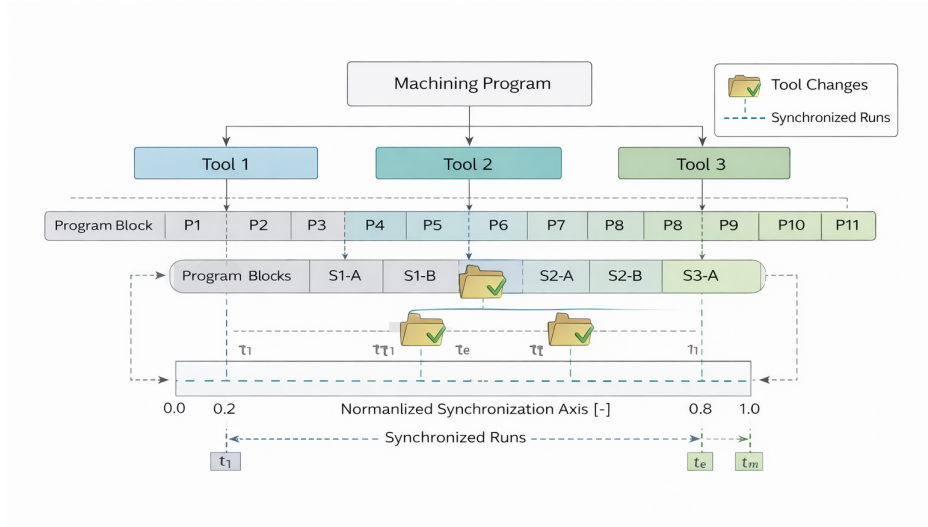


Figure 2. High-level organization of a machining program with tool changes and sub-program execution over time [26].

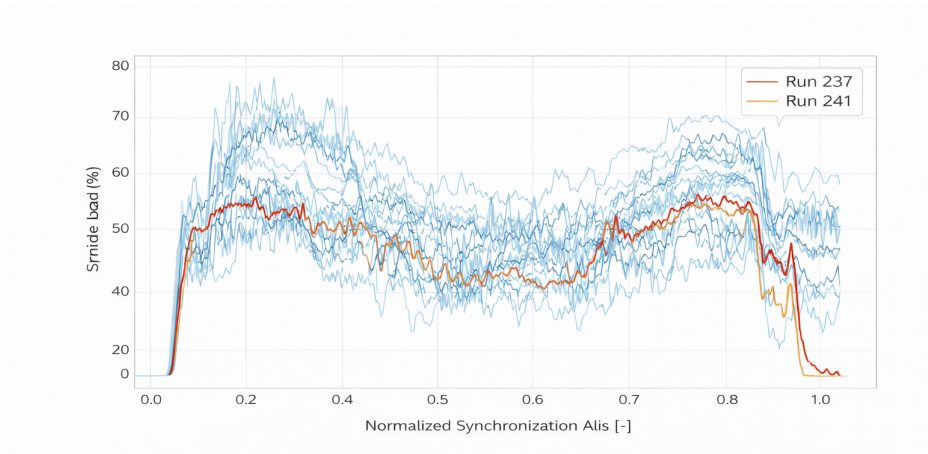


Figure 3. Synchronized spindle-load trajectories for the 18 runs of Program 1543, Tool 6040, and Machine T5-1; runs 237 and 241 are highlighted [26].

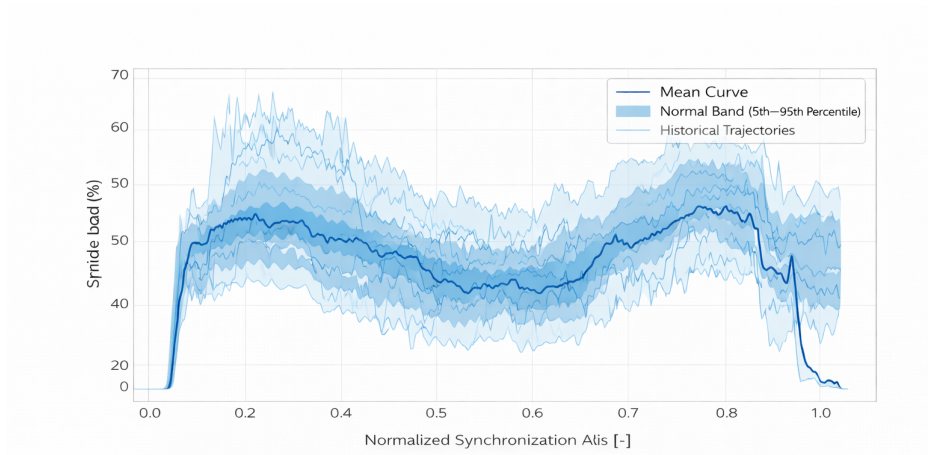


Figure 4. Mean spindle-load curve, 5th–95th percentile normal band, and historical trajectories for the aligned runs of Program 1543, Tool 6040, and Machine T5-1.

Table 2. Industrial dataset characteristics used in this study.

Characteristic	Description
Manufacturing domain	Aerospace machining of titanium parts
Primary monitoring variable	Spindle load from CNC controller
Acquisition rate	1/3 Hz
Signal structure	Repeated synchronized runs of a given program/tool combination
Analyzed program/tool/machine	Program 1543, tool 6040, machine T5-1
Number of reported runs in example	18 runs
Abnormal runs	237 and 241
Reference density-based method	Kernel density estimation with density-threshold monitoring
Industrial challenge	Low-rate, unsynchronized, heterogeneous controller data

3. Shape-Based FPCA Monitoring Method

3.1. Overview

A complete spindle-load trajectory $x_r(t)$ for run r at index t is considered as a single object instead of a collection of independent time-binned samples here. Specifically, let $x_r(t)$ be the spindle-load measurement at run r and time t , where $r = 1, 2, \dots, N$ and $t = 1, 2, \dots, T$. Since the shop-floor process executions vary slightly in length, all sequences are first rescaled along a standard process axis. The next step involves fitting a robust FPCA model to capture the dominating pattern of normal behavior, and analyzing the run based on its latent space representation and reconstruction error.

The monitoring pipeline consists of five interrelated steps which are compatible with the functional monitoring tradition, PCA-based statistical process control approaches, and batch trajectories. The steps are as follows:

1. Segmentation according to program and tooling,
2. Synchronization and rescaling of the trajectory length,
3. Smoothed functional data representation,
4. Robust FPCA of in-control data,
5. Run-level and local alarms using persistent homology-based criteria.

An overview of the workflow is shown in Figure 5, starting with the controller-level segmentation step and ending with run-level and local alarms for shop-floor interpreters.

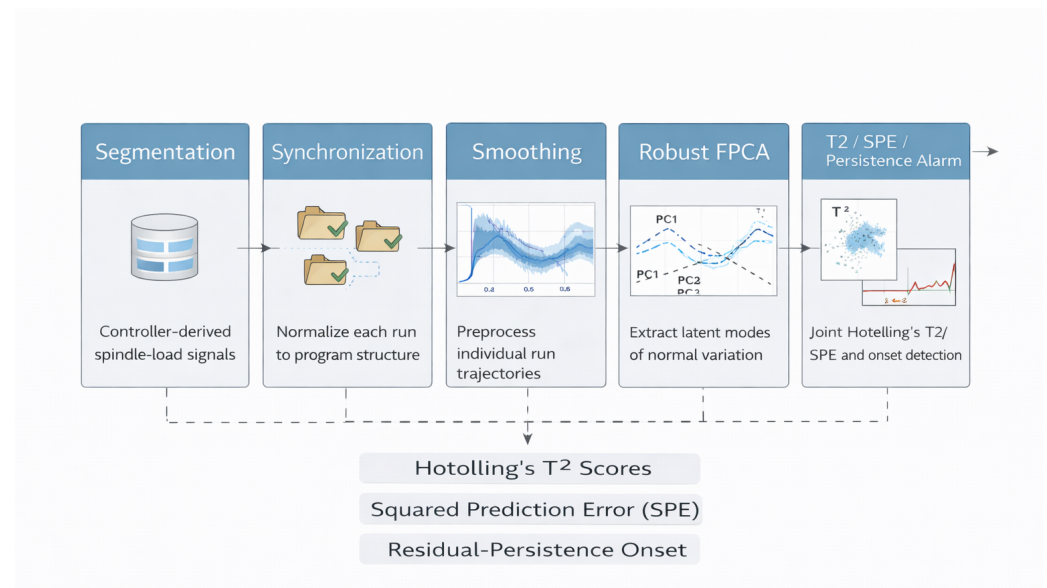


Figure 5. Robust FPCA monitoring workflow for low-sampling-rate spindle-load trajectories: segmentation, synchronization, smoothing, latent-space learning, and alarm generation.

3.2. Functional representation of spindle load runs

Once the synchronization procedure has been applied to the data, each spindle-load run can be represented as a function of the normalized time $\tau \in [0, 1]$. A light smoothing operation based on a cubic smoothing spline has been applied to the data to mitigate the staircase effect induced by the low sampling frequency while preserving the shape of the spindle-load run. Due to the low acquisition rate, the smoothing is very light. In such way, $\tilde{x}_r(\tau)$ represents the corresponding smoothed run on a common grid of T^* points.

In order to estimate the mean normal spindle-load trajectory, one should compute

$$\mu(\tau) = \frac{1}{N} \sum_{r=1}^N \tilde{x}_r(\tau), \quad (1)$$

where N is the number of historical runs used for the model creation. The centered spindle-load trajectories read

$$z_r(\tau) = \tilde{x}_r(\tau) - \mu(\tau). \quad (2)$$

It already reflects an important feature of the proposed technique: normal machining is not just a cloud of point-wise observations, but a curve fluctuating about a particular operational shape [?].

3.3. Robust functional principal component analysis

A centered functional curve can be described as a linear combination of orthonormal modes, i.e.,

$$z_r(\tau) \approx \sum_{k=1}^K a_{rk} \phi_k(\tau) + \epsilon_r(\tau), \quad (3)$$

where $z_r(\tau)$ represents a run r , $\phi_k(\tau)$ is the k -th principal component function, a_{rk} is the corresponding score coefficient of the run on this mode, K is the number of selected components, and $\epsilon_r(\tau)$ is the part that cannot be represented by the selected subspace.

The principal modes are calculated as eigenvectors of the empirical covariance of the functional dataset. Since we want the approach to be robust to noisy and borderline runs in the archive, especially when it is small and labels are not reliable, a robust alternative to the classical sample covariance estimator must be chosen [28]. To decide which K should be selected, the number of components retained until a particular threshold in explained variability is reached needs to be determined. This is usually set in the range from 90% to 95%:

$$\frac{\sum_{k=1}^K \lambda_k}{\sum_{k=1}^{T^*} \lambda_k} \geq \eta. \quad (4)$$

Here, K is the number of retained components and λ_k is the eigenvalue corresponding to ϕ_k .

As a result of the step above, one obtains a compact latent representation of the normal behavior of the process under study. The first principal component accounts for global amplitude differences, while the second one is responsible for shape bending or mismatch during the process. Further principal components account for smaller details. These modes may be analyzed by engineers and understood as certain deviations in operation. Figure 6 presents three modes of deformations used for interpreting latent bases for spindle load trajectories.

3.4. Run-level monitoring statistics

For a new run $\tilde{x}_{\text{new}}(\tau)$, the centered trajectory is projected onto the learned basis:

$$a_k = \int_0^1 (\tilde{x}_{\text{new}}(\tau) - \mu(\tau)) \phi_k(\tau) d\tau, \quad k = 1, \dots, K. \quad (5)$$

Two complementary monitoring statistics are then computed.

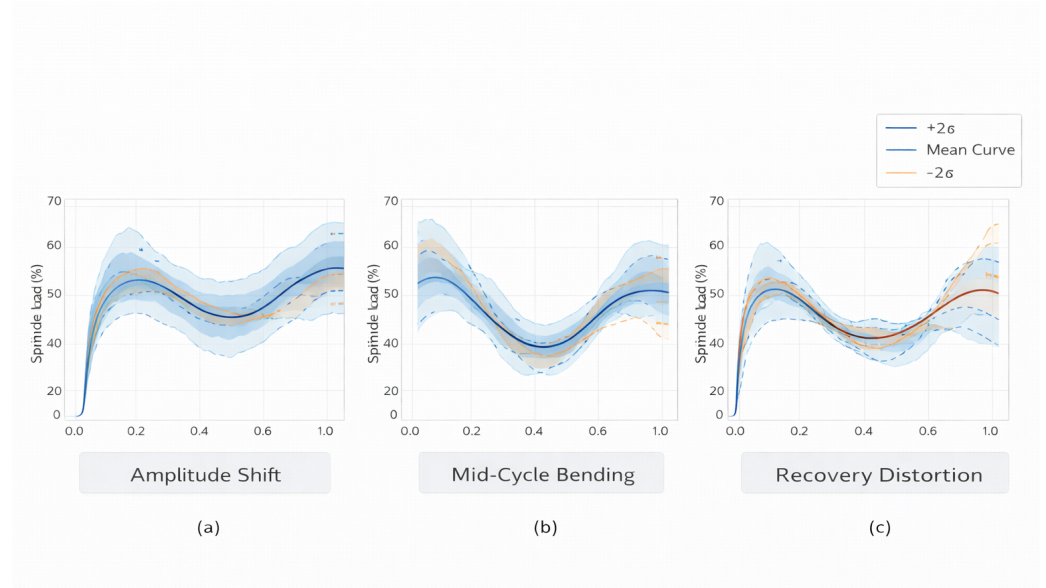


Figure 6. Dominant FPCA deformation patterns around the mean spindle-load profile: amplitude shift, mid-cycle bending, and recovery distortion.

3.4.1. Hotelling's T^2

The first measure quantifies the departure of the score vector from the center of the latent space, assumed to have a multivariate normal distribution:

$$T^2 = \mathbf{a}^\top \Lambda_K^{-1} \mathbf{a}, \quad (6)$$

where $\mathbf{a} = [a_1, \dots, a_K]^\top$ and $\Lambda_K = \text{diag}(\lambda_1, \dots, \lambda_K)$.

Large T^2 implies that the run appears anomalous relative to the nominal process even after being projected onto the latent space of nominal processes. That is, although the trajectory belongs to the same family as the nominal ones, it is situated at an extremely remote location within the family.

3.4.2. Squared prediction error

The second test checks how well the run can be approximated by the retained modes of variation:

$$\text{SPE} = \int_0^1 \left[\tilde{x}_{\text{new}}(\tau) - \mu(\tau) - \sum_{k=1}^K a_k \phi_k(\tau) \right]^2 d\tau. \quad (7)$$

If SPE takes on large values, then this means that the run contains some components that lie outside the space of normal modes. Such a criterion is helpful for identifying structurally anomalous runs, which cannot simply be considered the most extreme realization of the nominal process.

The pair (T^2, SPE) provides more information than a single anomaly score. For instance, a run with high T^2 but modest SPE may correspond to a strong yet familiar variation of the normal process, while a run with high SPE may reveal a genuinely new abnormal shape [19].

3.5. Local residual detection and alarm persistence

In industrial environments, a simple run alarm might not suffice; there is also a need to know when the process begins to deviate from its usual behavior. For this purpose, we define the local residual measure as follows:

$$d(t) = \frac{|x(t) - \hat{x}(t)|}{\hat{\sigma}(t) + \varepsilon}, \quad (8)$$

where $\hat{x}(t)$ is the FPCA reconstruction, $\hat{\sigma}(t)$ is the time-dependent standard deviation of the residuals obtained through historical normal runs, and ε is a constant used for numerical purposes.

The presence of a local warning signal implies that the value of $d(t)$ is above some threshold δ . To decrease the number of false alarms caused by noise or synchronization errors, a minimum of m consecutive time points must have this property before an anomaly is declared. Given the low-rate nature of the problem considered here, the values $m = 3$ to $m = 5$ can be expected, in accordance with the alarm logic employed in low-rate machining process control.

3.6. Estimating thresholds

Since industrial datasets are typically small, and cannot be assumed to be well-behaved in terms of distributions, the critical thresholds of T^2 , SPE, and $d(t)$ must be obtained via empirical analysis of the historical normal dataset [15]. Let q_{T^2} and q_{SPE} represent the 99th percentile levels of the in-control training distributions of T^2 and SPE []. Then, the new run is classified as an anomaly when

$$T^2 > q_{T^2} \quad \text{or} \quad \text{SPE} > q_{\text{SPE}}, \quad (9)$$

and the local departure criterion based on $d(t)$ is used to identify the approximate onset time of the anomaly.

Algorithm 1 FPCA monitoring procedure for low-rate spindle-load runs.

Require: Historical synchronized runs $\{x_r(t)\}_{r=1}^N$, new run $x_{\text{new}}(t)$

Ensure: Run-level alarm and local onset indication

- 1: Normalize all runs to a common process axis
 - 2: Lightly smooth and resample each run to fixed length T^*
 - 3: Compute the mean trajectory $\mu(\tau)$
 - 4: Estimate the robust covariance of centered runs
 - 5: Extract principal modes $\phi_k(\tau)$ and eigenvalues λ_k
 - 6: Select the smallest K satisfying the target explained variance
 - 7: Project $x_{\text{new}}(\tau)$ onto retained modes to obtain scores \mathbf{a}
 - 8: Compute T^2 using Eq. (6)
 - 9: Compute SPE using Eq. (7)
 - 10: Reconstruct the run $\hat{x}(t)$ and compute the local residual profile $d(t)$
 - 11: **if** $T^2 > q_{T^2}$ or $\text{SPE} > q_{\text{SPE}}$ **then**
 - 12: Mark the run as suspicious
 - 13: **end if**
 - 14: **if** $d(t) > \delta$ for at least m consecutive samples **then**
 - 15: Confirm the abnormal run and report the first sustained violation time
 - 16: **end if**
-

4. Results and Discussion

4.1. Normal operating manifold

The set of synchronized spindle-load trajectories for Program 1543, Tool 6040, and Machine T5-1 comprises a concentrated group exhibiting a steep early slope, a range of mid-cycle variation, and a final recovery stage, as depicted in Figure 3. The summary of this group by the mean trajectory and the 5th–95th percentile normal band is provided in Figure 4. This dataset is well-suited for FPCA since the principal components capture coherent trajectory characteristics and not individual events.

In the context of the dataset being considered here, the first FPCA mode represents the general level of spindle load, the second accounts for mid-cycle bending, and the third captures recovery distortion, as can be seen in Figure 6. Modes provide a reasonable characterization of acceptable variation in the manufacturing process under consideration.

This feature sets it apart from pointwise density mapping. While density maps can help us understand the location of the distribution at each aligned time, FPCA can help us understand the dynamics of changes across the entire trajectory and thereby help detect whether the suspicious trajectory is due to gradual drift or changes in onset behavior, or perhaps some other cause [27,32].

Figure 7 illustrates the differences between monitoring based on KDE applied to time bins and shape monitoring using FPCA for the spindle-load trajectories aligned in time.

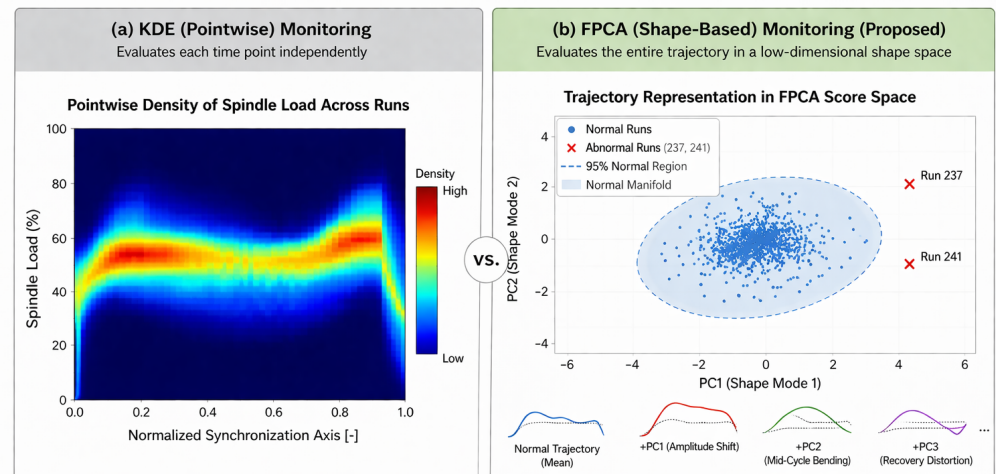


Figure 7. Time-bin-wise KDE monitoring and FPCA-based shape monitoring for the aligned spindle-load trajectories.

4.2. Anomalous Runs 237 and 241

Among the 18 runs, runs 237 and 241 appear to be the two most anomalous runs based on the reference analysis performed through density clustering, which yielded average values of 47.52% and 45.34%, respectively. These runs were observed to exhibit sustained abnormal behavior from around 189 s and 303 s, respectively.

These results corroborate the conclusions made using the FPCA framework. For example, run 237 starts exhibiting abnormal behavior sooner than run 241. As explained by Nomikos [19], in the context of FPCA, an anomaly may be seen as either large displacement in score space or a large reconstruction residual or both.

Figure 8, 9, and 10, along with Table 3, serve as complementary evidence to show the anomalies. Specifically, score space illustrates geometric separation in the retained latent space, while residual persistence focuses on the onset of persistent abnormality. The integrated diagnostic summary incorporates spindle load evolution and monitoring statistic. Thus, the results indicate that runs 237 and 241 are trajectories rather than local anomalies [33].

The above figures illustrate the residual-persistence behavior and the onsets at 189 s and 303 s for runs 237 and 241. The figure below gives an integrated summary of the spindle load evolution and monitoring statistic behavior for runs 237 and 241 in a single plot.

4.3. Advantages of using a shape-based model in low sampling rate

When the sampling rate is low, as it is here with one sample per three seconds, the dynamics of the process trajectory can no longer be characterized in terms of high-frequency transients or any other frequency domain characteristics. It is now the shape of the function which is relevant in assessing stability of the machine. Relevant features include rapidity with which spindle load grows in the beginning, stabilization of the process trajectory at the expected levels, depth of the valleys, and similarity of the trajectory shape in the latter stages to the historical ones.

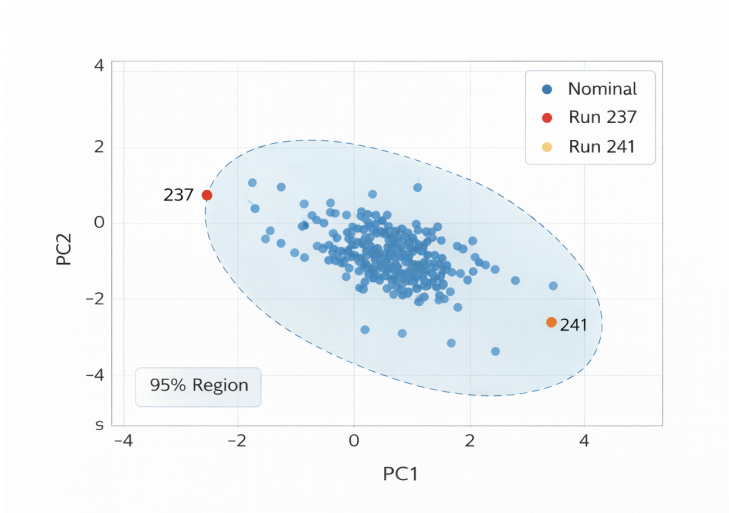


Figure 8. Score-space separation of the 18 synchronized runs, showing the displaced positions of runs 237 and 241 in the retained FPCA manifold.

Table 3. Density-based run scores for the 18 synchronized runs; lower scores indicate more abnormal behavior [26].

Run	Score (%)	Run	Score (%)
69	68.37	233	80.00
73	74.47	237	47.52
89	51.89	241	45.34
93	73.47	320	63.22
127	63.26	324	63.93
131	59.03	328	73.30
135	80.28	354	68.85
186	77.47	356	77.91
190	80.13		
194	56.44		

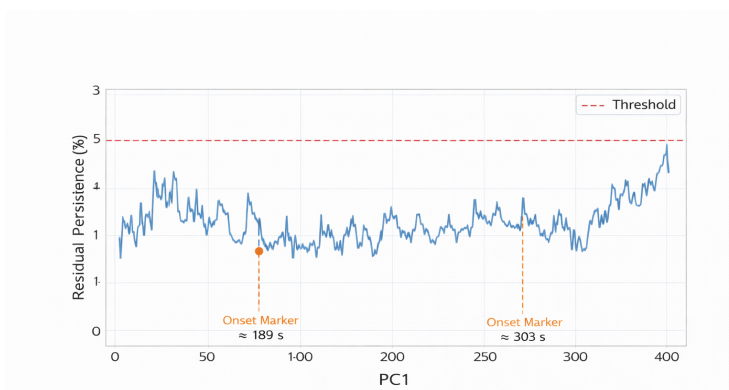


Figure 9. Illustration of residual-persistence onset detection for runs 237 and 241, indicating long-term deviations around 189 s and 303 s.

The advantage of FPCA in low sampling rate regimes is obvious, since FPCA operates on the entire trajectory directly. Moreover, FPCA compresses data dimensions without losing time dependency. Hence, in the industrial implementation scenario discussed above, very little model memory is needed. Namely, the mean function, few modes of the trajectory, and some threshold values are sufficient. Finally, computations associated with monitoring

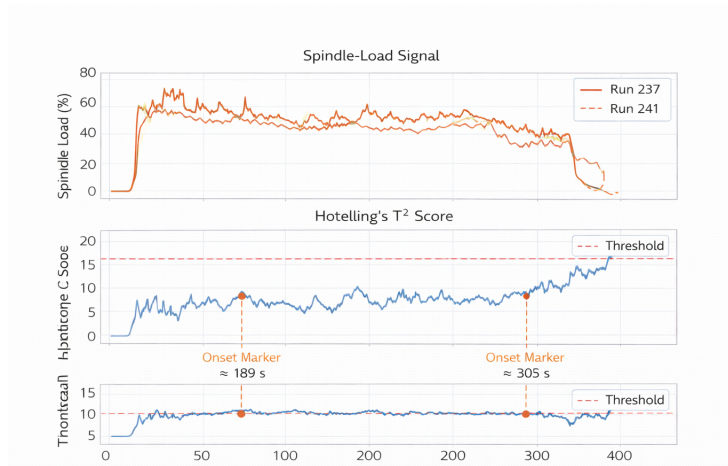


Figure 10. Integrated diagnostic summary for runs 237 and 241, combining spindle-load evolution with monitoring-statistic trends and onset markers.

of new run consist mostly of projections and residuals calculation, hence, are relatively cheap compared to learning-oriented data-driven models.

4.4. Comparison with the KDE approach

The density-based model and the FPCA model used in this paper are compared below in Table 4. In addition, Figure 7 provides a visual illustration of the difference between pointwise density monitoring and trajectory space monitoring.

Table 4. Comparison between density-based monitoring and FPCA-based trajectory model used in this paper.

Aspect	Density-based monitoring (KDE)	FPCA monitoring in this study
Basic representation	Local spindle-load density	Trajectory of the entire run
Principal strength	Local probability envelope	Trajectory shape
Interpretation	Normal region for each time bin	Trajectory mean and dominant shape modes
Taking correlation across time into account	Indirectly	Directly, through functional modes
Anomaly identification	Local outliers	Extreme deviations or bad reconstruction in score space
Storage demands	Local density models for all time bins	Mean trajectory, basis functions and thresholds
Suitability for low sampling rates	Good	Excellent if the trajectory shape carries most information
Potential pitfall	Underutilization of run structure	Careful selection of basis functions needed

4.5. Methodological significance

In terms of methodology, the key improvement of the current approach lies in its shift from density check on the local scale to structural analysis at the level of individual runs. The use of both T^2 and SPE allows us to differentiate between atypical runs that can still be reconstructed using our learned normal manifold and runs that possess shape characteristics that cannot be captured by the latter. Persistence of the residual further introduces a notion of temporal localization into the picture, allowing the model to retain an overarching view while still specifying the start of the sustained deviation. All of the above features become possible due to the use of controller-only synchronization and the resulting possibility to calculate the necessary values based on that trace only.

5. Industrial Deployment Considerations

Industrial applicability is one of the decisive factors when it comes to choosing an adequate monitoring technique for manufacturing purposes. Since the proposed FPCA-based model relies on spindle load data obtained via controllers only, it does not incur costs associated with installing high-frequency sensors; the training procedure and model calibration are efficient and relatively quick, and on-line evaluation reduces to simple projections. That said, certain conditions should be met to ensure good performance in the industrial environment.

First, similarly to any data-driven approach, our model assumes availability of a representative sample of normal runs. Any changes in production, including switching tools, changing the cutting regime, or modifying the CNC program, will necessitate retraining. Second, synchronization plays a crucial role for the proposed model, as the accuracy of it might otherwise lead to artificially elevated residuals. Finally, as the whole database of controller records belongs to the manufacturer, the analysis is currently limited to the synchronization cases included in our sample. Still, despite those limitations, the model fits the reality of industrial environment quite well.

Despite the limitations, the trajectory model is still applicable to real-world settings. Factories cannot afford to have dense sensing and sophisticated data engineering pipelines along with complex algorithms for learning. In such a scenario, a model based on sparse sensing and learning is a good balance point.

6. Conclusion

In this paper, we have presented an approach to CNC machine monitoring based on shape-based functional principal component analysis with spindle load trajectory synchronization. Our study focused on 18 runs for Program 1543, Tool 6040, and Machine T5-1, where the sampling rate was set to 1/3 Hz, and we used the two recorded abnormal runs 237 and 241 as examples of runs requiring engineering attention. Rather than using a separate normality decision criterion at each time bin, we propose modeling runs as functional trajectories and estimating a low-dimensional normal manifold. Hotelling's T^2 statistic combined with the squared prediction error helps distinguish between anomalies characterized by unusual placement in relation to normal data points and anomalies with an unusual shape relative to the estimated normal basis. Additionally, the local residual profile and the persistence rule give an easy way to compute the estimated time at which anomalies arise. Based on our findings, the applicability of FPCA depends on whether the process of interest is best characterized by trajectory shape or transients. Future research could investigate applying our proposed methods to complete controller archives, compare with the KDE reference directly, as well as explore multivariate trajectory monitoring techniques incorporating spindle load, feed load, spindle speed, and vibration data. Nevertheless, even with the current limitations, this research demonstrates the robustness of FPCA as an alternative approach to monitoring CNC machining processes when compared with pointwise KDE.

References

- [1] Tao, F., Qi, Q., Liu, A., &Kusiak, A. (2018). Data-driven smart manufacturing. *Journal of manufacturing systems*, 48, 157-169.
- [2] Wang, J., Ma, Y., Zhang, L., Gao, R. X., &Wu, D. (2018). Deep learning for smart manufacturing: Methods and applications. *Journal of manufacturing systems*, 48, 144-156.
- [3] Baur, M., Albertelli, P., &Monno, M. (2020). A review of prognostics and health management of machine tools. *The International Journal of Advanced Manufacturing Technology*, 107(5), 2843-2863.
- [4] Mohanraj, T., Shankar, S., Rajasekar, R., Sakthivel, N. R., &Pramanik, A. (2020). Tool condition monitoring techniques in milling process—A review. *Journal of Materials Research and Technology*, 9(1), 1032-1042.
- [5] Teti, R., Jemielniak, K., O'Donnell, G., &Dornfeld, D. (2010). Advanced monitoring of machining operations. *CIRP annals*, 59(2), 717-739.
- [6] Byrne, G., Dornfeld, D., Inasaki, I., Ketteler, G., König, W., &Teti, R. (1995). Tool condition monitoring (TCM)—the status of research and industrial application. *CIRP annals*, 44(2), 541-567.
- [7] Snr, D. E. D. (2000). Sensor signals for tool-wear monitoring in metal cutting operations—a review of methods. *International journal of machine tools and manufacture*, 40(8), 1073-1098.
- [8] Sick, B. (2002). On-line and indirect tool wear monitoring in turning with artificial neural networks: a review of more than a decade of research. *Mechanical systems and signal processing*, 16(4), 487-546.
- [9] Rehorn, A. G., Jiang, J., &Orban, P. E. (2005). State-of-the-art methods and results in tool condition monitoring: a review. *The International Journal of Advanced Manufacturing Technology*, 26(7), 693-710.
- [10] Dutta, S., Pal, S. K., Mukhopadhyay, S., &Sen, R. (2013). Application of digital image processing in tool condition monitoring: A review. *CIRP Journal of Manufacturing Science and Technology*, 6(3), 212-232.
- [11] Zhou, Y., &Xue, W. (2018). Review of tool condition monitoring methods in milling processes. *The International Journal of Advanced Manufacturing Technology*, 96(5), 2509-2523.

- [12] Jemielniak, K. (1999). Commercial tool condition monitoring systems. *The International Journal of Advanced Manufacturing Technology*, 15(10), 711-721.
- [13] Jantunen, E. (2002). A summary of methods applied to tool condition monitoring in drilling. *International Journal of Machine Tools and Manufacture*, 42(9), 997-1010.
- [14] Ambhore, N., Kamble, D., Chinchani, S., &Wayal, V. (2015). Tool condition monitoring system: A review. *Materials Today: Proceedings*, 2(4-5), 3419-3428.
- [15] Jackson, J. E., &Mudholkar, G. S. (1979). Control procedures for residuals associated with principal component analysis. *Technometrics*, 21(3), 341-349.
- [16] Kourti, T., &MacGregor, J. F. (1995). Process analysis, monitoring and diagnosis, using multivariate projection methods. *Chemometrics and intelligent laboratory systems*, 28(1), 3-21.
- [17] Kosanovich, K. A., Dahl, K. S., &Piovoso, M. J. (1996). Improved process understanding using multiway principal component analysis. *Industrial &engineering chemistry research*, 35(1), 138-146.
- [18] Nomikos, P., &MacGregor, J. F. (1994). Monitoring batch processes using multiway principal component analysis. *AIChE Journal*, 40(8), 1361-1375.
- [19] Nomikos, P., &MacGregor, J. F. (1995). Multivariate SPC charts for monitoring batch processes. *Technometrics*, 37(1), 41-59.
- [20] Ku, W., Storer, R. H., &Georgakis, C. (1995). Disturbance detection and isolation by dynamic principal component analysis. *Chemometrics and intelligent laboratory systems*, 30(1), 179-196.
- [21] Louwerse, D. J., &Smilde, A. K. (2000). Multivariate statistical process control of batch processes based on three-way models. *Chemical Engineering Science*, 55(7), 1225-1235.
- [22] Chen, J., &Liu, K. C. (2002). On-line batch process monitoring using dynamic PCA and dynamic PLS models. *Chemical Engineering Science*, 57(1), 63-75.
- [23] Venkatasubramanian, V., Rengaswamy, R., Yin, K., &Kavuri, S. N. (2003). A review of process fault detection and diagnosis: Part I: Quantitative model-based methods. *Computers &chemical engineering*, 27(3), 293-311.
- [24] Venkatasubramanian, V., Rengaswamy, R., &Kavuri, S. N. (2003). A review of process fault detection and diagnosis: Part II: Qualitative models and search strategies. *Computers &chemical engineering*, 27(3), 313-326.
- [25] Venkatasubramanian, V., Rengaswamy, R., Kavuri, S. N., &Yin, K. (2003). A review of process fault detection and diagnosis: Part III: Process history based methods. *Computers &chemical engineering*, 27(3), 327-346.
- [26] Bernard, G., Achiche, S., Girard, S., &Mayer, R. (2021). Condition monitoring of manufacturing processes under low sampling rate. *Journal of Manufacturing and Materials Processing*, 5(1), 26.
- [27] Lee, W. J., Mendis, G. P., Triebe, M. J., &Sutherland, J. W. (2020). Monitoring of a machining process using kernel principal component analysis and kernel density estimation. *Journal of Intelligent Manufacturing*, 31(5), 1175-1189.
- [28] Hubert, M., Rousseeuw, P. J., &Vanden Branden, K. (2005). ROBPCA: a new approach to robust principal component analysis. *Technometrics*, 47(1), 64-79.
- [29] Ruppert, D. (2004). *The elements of statistical learning: data mining, inference, and prediction*.
- [30] Aggarwal, C. C. (2016). An introduction to outlier analysis. In *Outlier analysis* (pp. 1-34). Cham: Springer International Publishing.
- [31] Altintas, Y., &Ber, A. A. (2001). Manufacturing automation: metal cutting mechanics, machine tool vibrations, and CNC design. *Appl. Mech. Rev.*, 54(5), B84-B84.
- [32] Zhang, F., Liu, Y., Chen, C., Li, Y. F., &Huang, H. Z. (2014). Fault diagnosis of rotating machinery based on kernel density estimation and Kullback-Leibler divergence. *Journal of Mechanical Science and Technology*, 28(11), 4441-4454.
- [33] Joe Qin, S. (2003). Statistical process monitoring: basics and beyond. *Journal of Chemometrics: A Journal of the Chemometrics Society*, 17(8-9), 480-502.